A guanine nucleotide exchange factor (GEF) limits Rab GTPase–driven membrane fusion

Received for publication, August 17, 2017, and in revised form, November 14, 2017 Published, Papers in Press, November 28, 2017, DOI 10.1074/jbc.M117.812941

Lars Langemeyer[‡], **Angela Perz**[‡], **Daniel Kümmel**[§], **and Christian Ungermann**[‡1]

From the [‡]*Biochemistry Section and* [§]*Structural Biochemistry, Department of Biology/Chemistry, University of Osnabrück, Barbarastrasse 13, 49076 Osnabrück, Germany*

Edited by Karen G. Fleming

The identity of organelles in the endomembrane system of any eukaryotic cell critically depends on the correctly localized Rab GTPase, which binds effectors and thus promotes membrane remodeling or fusion. However, it is still unresolved which factors are required and therefore define the localization of the correct fusion machinery. Using SNARE-decorated proteoliposomes that cannot fuse on their own, we now demonstrate that full fusion activity can be achieved by just four soluble factors: a soluble SNARE (Vam7), a guanine nucleotide exchange factor (GEF, Mon1–Ccz1), a Rab–GDP dissociation inhibitor (GDI) complex (prenylated Ypt7–GDI), and a Rab effector complex (HOPS). Our findings reveal that the GEF Mon1–Ccz1 is necessary and sufficient for stabilizing prenylated Ypt7 on membranes. HOPS binding to Ypt7-GTP then drives SNARE-mediated fusion, which is fully GTP-dependent. We conclude that an entire fusion cascade can be controlled by a GEF.

Organelles of the endomembrane system continuously exchange membranes by fusion and fission reactions but maintain their overall identity. Rab GTPases cooperate with specific tethering complexes and organize the fusion of vesicles with organelles through membrane-localized SNAREs and thereby serve as signposts of organelle identity (1, 2). Newly made Rabs are posttranslationally lipidated by a geranylgeranyl transferase complex and kept soluble thereafter by a Rab escort protein (REP),[2] which binds both the GTPase domain and the hydrophobic hydrocarbon tail (3). After delivery to the right membrane, which is paralleled by REP release, a Rab-specific GEF promotes GTP loading on the organelle surface. This enables the Rab to bind to specific effectors and promote fusion (2, 4, 5). Turnover of Rabs on membranes requires a GTPase-activating protein, which completes the active catalytic site and stimulates GTP hydrolysis. The resulting Rab–GDP can then be either reactivated or extracted by the GDI, a functional homolog of REP (6), allowing for another cycle of membrane delivery and activation.

The exchange of consecutively acting Rabs as part of vesicle and organelle maturation is an essential part of organelle biogenesis both in exocytosis and endocytosis (2, 7–11). Such a process requires coordination between Rab recruitment and activation and subsequent inactivation of the previous Rab, a process named Rab cascade (12).

Despite extensive structural insights into Rab interactions with its regulators, the molecular mechanism of specific delivery of Rabs to the right surface is still poorly understood. Previous studies suggested that organelle-specific proteins other than GEFs are needed to determine efficient Rab delivery to membranes (13–18). However, GEFs that are relocalized to mitochondria *in vivo* also recruit their corresponding Rab (5, 19, 20), and, *in vitro*, GEFs can drive Rab delivery and activation on liposomes (21). Although this puts GEFs into the center, it remains unclear whether other cytosolic or membrane-bound factors may be involved in Rab localization during an authentic membrane fusion process.

To understand the underlying principles, we set out to determine the minimal machinery of Rab delivery, activation, and effector recruitment to membranes. We now present the functional reconstitution of Rab-driven membrane tethering and subsequent fusion based on just four soluble factors. Our data unravel the simplicity of how an organelle can become fusion-competent during its maturation and illustrate the importance of the correct spatiotemporal localization of GEFs.

Results

Activation of purified prenylated Ypt7 and Vps21

Organelles such as endosomes recruit Rabs from a cytosolic pool to their surface. To recapitulate this process *in vitro* and unravel the required components, we established protocols to generate functional Rab–REP or Rab–GDI complexes with the yeast Rab5 (Vps21) and Rab7 (Ypt7) using the published prenylation machinery of the two Rab geranylgeranyl transferase subunits Bet2 and Bet4, REP (Mrs6), GDI (Gdi1) (for all purified proteins, see Fig. S1), and geranylgeranyl pyrophosphate (21–23). We routinely obtained up to 90% prenylation in our reactions (Fig. 1*A*). Initially, we tested membrane association of the

This work was supported by SFB 944 Project P11 (to C.U.) and Project P18 (to D.K.) and an incentive award of the Department of Biology/Chemistry of the University of Osnabrück (to L.L.). The authors declare that they have no conflicts of interest with the contents of this article.

This article contains Figs. S1 and S2.

[1] To whom correspondence should be addressed: Fax: 49-541-969-2884 or 3422; E-mail: cu@uos.de.

[2] The abbreviations used are: REP, Rab escort protein; GEF, guanine nucleotide exchange factor; GDI, GDP dissociation inhibitor; DOGS-NTA, 1,2-dioleoyl-*sn*-glycero-3-[(N-(5-amino-1-carboxypentyl)iminodiacetic acid)succinyl]; GGPP, geranylgeranyl pyrophosphate; TEV, tobacco etch virus; GGTase, geranylgeranyltransferase; RPL, reconstituted proteoliposome; MANT-GDP, 2′/3′-*O*-(*N*-methyl-anthraniloyl)-guanosine-5′-diphosphate; α-SNAP, soluble *N*-ethylmaleimide fusion protein; NSF, *N*-ethylmaleimide–sensitive fusion protein; TAP, tandem affinity purification; HOPS, homotypic fusion and vacuole protein sorting; TRAPP, transport protein particle.

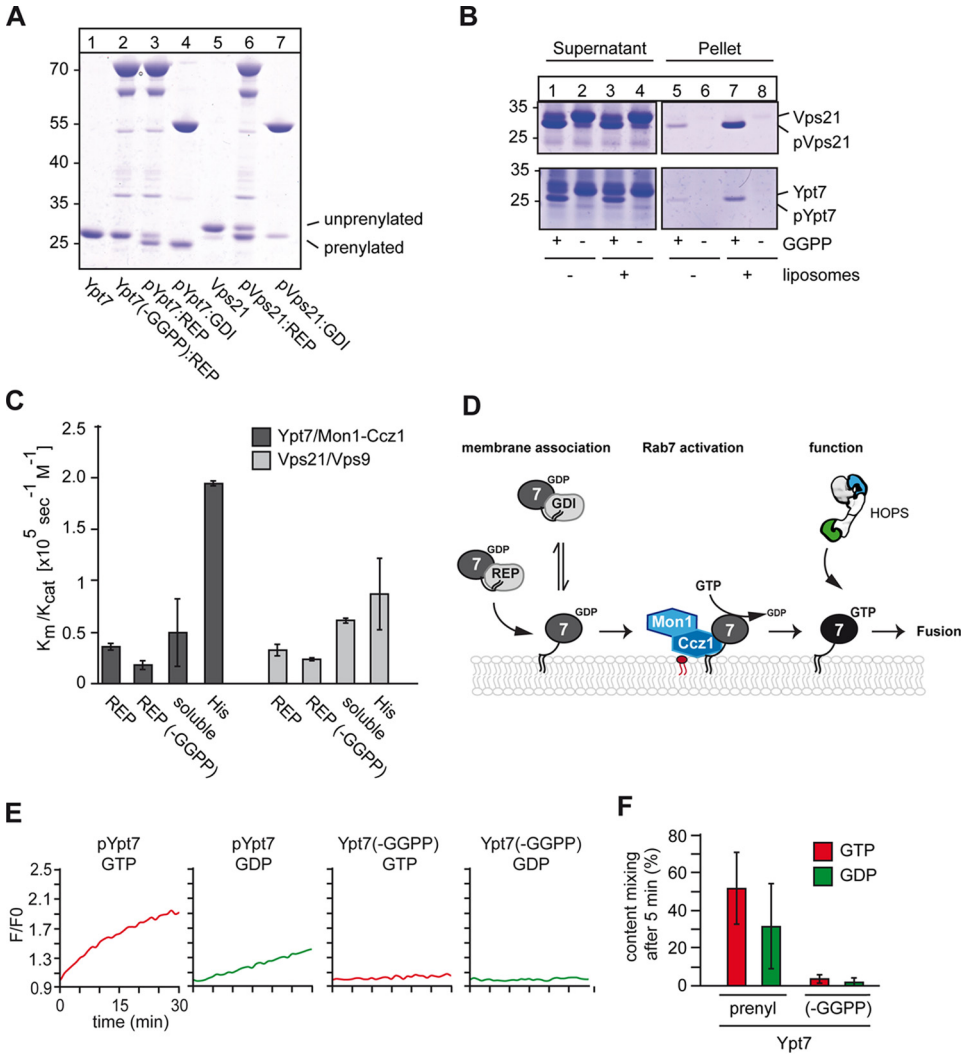

Figure 1. Establishment of *in vitro* prenylation and functionality of Ypt7 and Vps21. *A,* prenylation of Ypt7 and Vps21 *in vitro*. 3 μM Ypt7 or Vps21, respectively, 3 μM REP (Mrs6), 1 μM geranylgeranyltransferase (GGTase, Bet2-Bet4) were incubated with or without geranylgeranyl pyrophosphate (GGPP) at 30 °C for 30 min. Rab–GDI complexes were obtained as described previously (10). Samples were analyzed by SDS-PAGE and Coomassie staining. *B*, membrane association of Rabs after prenylation. Vps21 (*top*) and Ypt7 (*bottom*) were incubated with the prenylation machinery in either the presence or absence of GGPP as described in *A*. Where indicated, liposomes were added. To allow for membrane insertion after prenylation, the samples were incubated for another 30 min at 30 °C and then centrifuged for 30 min at 20,000 × *g*. The supernatant and pellet were analyzed by SDS-PAGE and Coomassie staining. *C*, analysis of GEF activity. 50 pmol of MANT–GDP–loaded Rabs were incubated with the respective GEF as described under "Materials and methods." Loss of fluorescence was monitored in a plate reader after addition of GTP to a final concentration of 0.1 mM for 30 min at 30 °C. GEF activity of the corresponding GEF toward prenylated (*REP*) and unprenylated (*REP* (−*GGPP*)) Rab–REP complexes was measured in the presence of liposomes. GEF assays with soluble Rabs were performed in the absence of liposomes using the corresponding GEF. C-terminally His-tagged Ypt7 and Vps21 (*His*) were incubated with their respective GEF in the presence of liposomes carrying DOGS-NTA. A summary of k_{cat}/K_m values was obtained from three different experiments. *D*, model of Mon1–Ccz1–dependent Rab recruitment to membranes. For details see text. *E* and *F*, analysis of RPL fusion. 160 nM prenylated or non-prenylated Ypt7–REP complex was added in the presence of 100 nM Mon1–Ccz1 and either GDP or GTP prior to starting fusion reactions to dye-loaded proteoliposomes. Proteoliposomes carried either the vacuolar SNAREs Vam3 and Vti1 or the R-SNARE Nyv1. The SNARE:lipid ratio was 1:10,000 (see "Materials and methods"). Fusion reactions were carried out in a plate reader for 30 min at 27 °C in the presence of a fusion mixture containing HOPS, Sec17, Sec18, Vam7, and ATP. After addition of the fusion mixture to each reaction, the FRET signal as a result of content mixing was recorded ($n = 3$).

Rab–REP complexes and observed spontaneous partitioning of only the prenylated Ypt7 (pYpt7) and Vps21 (pVps21) into protein-free liposomes (Fig. 1*B*). To test for functionality, we used liposome-bound Rabs to monitor their GEF-dependent activation. For this, we preloaded the prenylated Rabs Ypt7 and Vps21 with MANT–GDP and recorded the loss of fluorescence upon nucleotide exchange (24, 25). We observed efficient activation of Rabs regardless of their prenylation or the presence of REP (Fig. 1*C*). Only when His-tagged Rabs were directly bound to liposomes carrying DOGS-NTA, Rabs were activated with higher efficiency, as reported before (21, 25). We thus conclude that the *in vitro* prenylated Rabs can be recognized and activated by the corresponding GEF protein.

Prenylated Ypt7 drives membrane fusion

To test whether the prenylated Rab can drive an authentic fusion reaction, we focused on the vacuolar Rab Ypt7 in the context of reconstituted vacuole fusion. Previous studies established that proteoliposomes carrying vacuolar SNAREs with transmembrane domains and co-reconstituted prenylated Ypt7, purified from yeast cells, can fuse in the presence of the soluble SNARE Vam7, the SNARE chaperones Sec17/α-SNAP

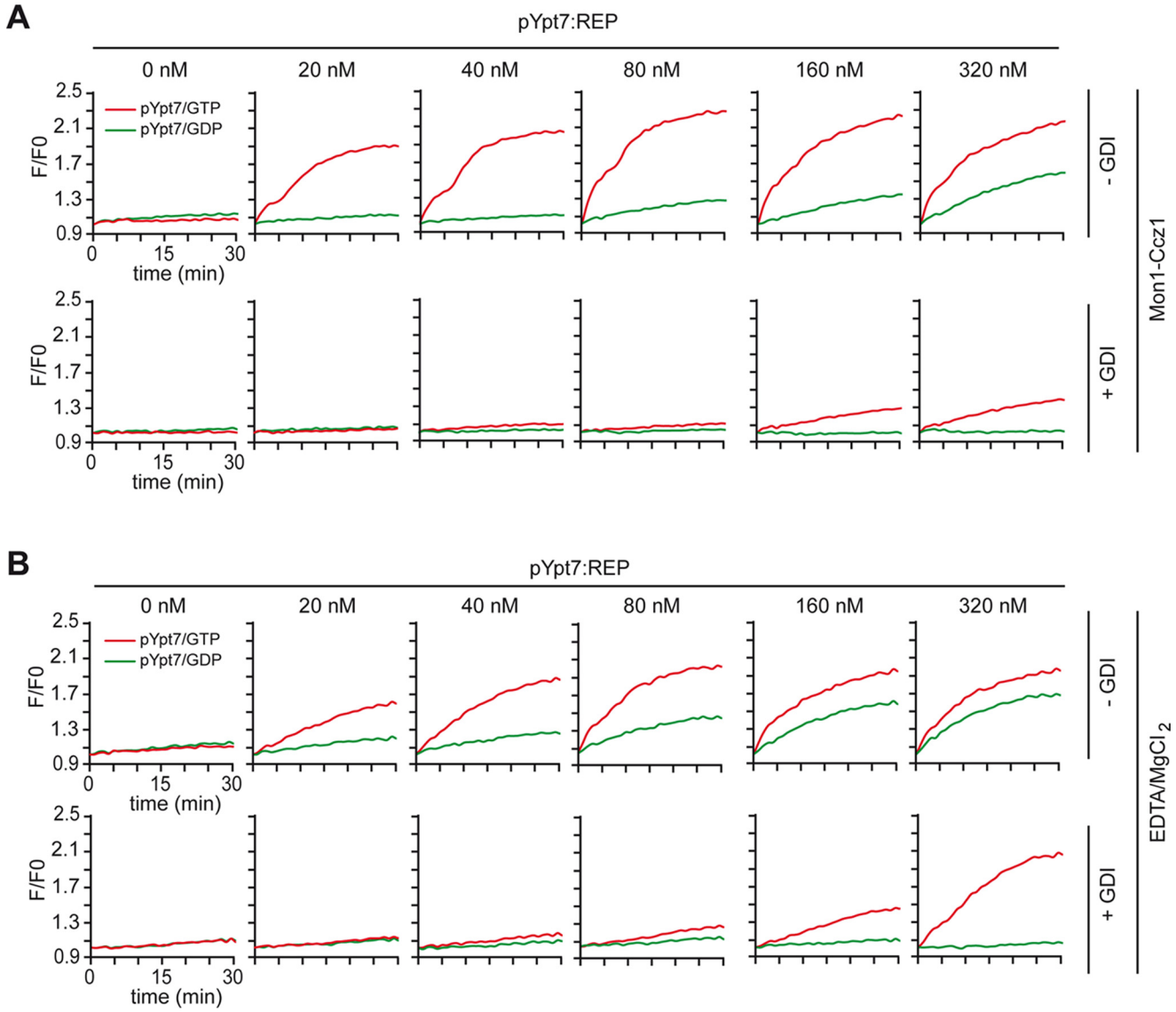

Figure 2. Reconstitution of GEF-driven Ypt7–REP activation and membrane fusion. *A*, GEF-mediated activation of prenylated Ypt7 in fusion. *Top panels*, 100 nM Mon1–Ccz1 complex was added to proteoliposomes and increasing amounts of prenylated Ypt7–REP and preincubated for 15 min at 27 °C before addition of the fusion mix. *Bottom panels*, 500 nM GDI was added 10 min after starting the nucleotide exchange. *B*, EDTA-driven activation of prenylated Ypt7 in fusion. 2 mM EDTA and, after 10 min incubation, 3 mM $MgCl_2$ were used to drive nucleotide exchange. Fusion was measured in the absence (*top panels*) or presence (*bottom panels*) of 500 nM GDI as in *A*. Curves shown for content mixing assays are representatives of at least three independent experiments, using differing amounts of Ypt7, which led to the same overall result.

and Sec18/NSF, which activate SNAREs in the presence of ATP, and the HOPS tethering complex (26–28). HOPS binds to Ypt7 on both membranes to drive tethering and assemble SNAREs (29–32) (Fig. 1*D*). Fusion was assayed by mixing of the luminal dyes biotin–phycoerythrin and Cy5-streptavidin, present in separate tester liposomes, which produce a strong FRET signal after luminal mixing (26).

We used previously established conditions of optimized lipid composition and physiological SNARE concentrations, which makes fusion entirely Ypt7- and HOPS-dependent (33, 34). We also used a heterotypic fusion assay, where the Q_a and Q_b SNAREs Vam3 and Vti1 reside on one membrane, whereas the R-SNARE Nyv1 is on the other proteoliposome (Fig. S2). However, we now omitted prenylated Ypt7 from the reconstitution but provided the prenylated Rab as a soluble factor, either in complex with REP or GDI. Thus, fusion should depend exclusively on the added Ypt7 but should require its GEF Mon1–Ccz1, which was included in our fusion assays.

We initially titrated the Ypt7–REP complex to the fusion reaction, which was generated either in the presence or absence of GGPP. Only prenylated Ypt7 was able to support fusion, indicating that our prenylated Ypt7 is fully functional (Fig. 1, *E* and *F*). We noticed that fusion was also observed in the presence of GDP, as reported previously (27, 34). We therefore extended our titration of pYpt7–REP to the fusion assay and observed clear GTP dependence at lower pYpt7–REP concentrations, whereas, at higher concentrations, both GDP and GTP stimulated fusion equally (Fig. 2*A*, *top panels*). HOPS also binds GDP-loaded Ypt7 *in vitro* (32, 34). However, cells possess GDI to extract GDP-loaded Rabs (35). Indeed, when GDI was included, GDP-dependent fusion was strongly suppressed (Fig. 2*A*, *bottom panels*).

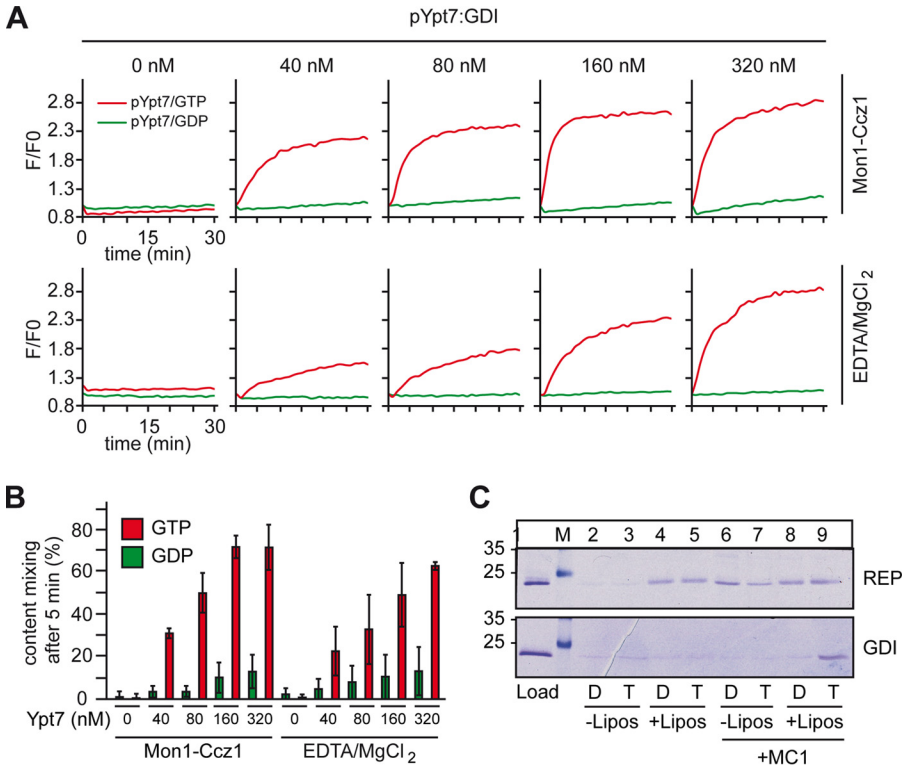

Figure 3. Reconstitution of GEF-driven Ypt7–GDI activation and membrane fusion. *A* and *B*, the Ypt7–GDI complex was titrated into the fusion assay as in Fig. 2, and nucleotide exchange was either driven by Mon1–Ccz1 (*top panels*) or EDTA/$MgCl^{2+}$ (*bottom panels*). GTP or GDP was added as indicated. *C*, membrane association of pYpt7 in complex with REP (*top panel*) or GDI (*bottom panel*). To allow for membrane insertion, samples were incubated in either the presence or absence of liposomes, GDP (*D*) or GTP (*T*), and, where indicated, with Mon1–Ccz1 for 30 min at 30 °C and then centrifuged for 30 min at 20,000 × *g*. The supernatant and pellet were analyzed by SDS-PAGE and Coomassie staining (representative example, $n = 3$).

To ask whether recruitment of prenylated Ypt7 onto membranes occurs exclusively by the corresponding Mon1–Ccz1 complex, we triggered nucleotide exchange by EDTA and Mg^{2+} and observed the same Ypt7 triggered fusion as before (Fig. 2*B*). GDP-dependent fusion was likewise suppressed by addition of GDI. We noticed that, after addition of GDI, more pYpt7–REP complex was required to obtain the same fusion as observed in the absence of GDI. This indicates that the combination of GEF and GDI restricts the pool of readily available Ypt7 for fusion.

A GEF can act as a limiting factor to recruit pYpt7 for fusion

In the cell, cytosolic Rabs are in complex with GDI. We therefore tested the pYpt7–GDI complex to drive liposome fusion. With GDP as a nucleotide, no fusion was observed, regardless of whether we increased the amount of pYpt7–GDI complex (Fig. 3, *A*, *top panels*, *green lines*, and *B*). However, in the presence of GTP, robust fusion was observed (Fig. 3*A*, *top panel*, *red lines*; quantified in Fig. 3*B*). This strongly differs from our observations of the pYpt7–REP complex (Fig. 2, *A* and *B*). When we used Mg^{2+} and EDTA instead of GEF, fusion was as efficient (Fig. 3*A*, *bottom panels*; quantified in Fig. 3*B*).

The analysis of the membrane association of pYpt7–REP and pYpt7–GDI in the presence or absence of Mon1–Ccz1 clearly illustrates the reason for the difference seen in the fusion assays (Fig. 3*C*). Although pYpt7–REP allows for spontaneous membrane association of the Rab GTPase, as observed before (Fig. 1*B*), pYpt7 bound to GDI only inserted into the membrane in the presence of both its GEF and GTP. Noteworthy is that the amount of Ypt7 associating with membranes from the REP complex did not increase in the presence of the GEF and GTP. This strongly suggests that the required GEF, Mon1–Ccz1, could be limiting in the course of events that finally lead to fusion.

To test for the minimal requirements of pYpt7–GDI– dependent fusion, we selectively omitted each of the fusion components from the assay. Fusion was entirely blocked without pYpt7–GDI, Mon1–Ccz1, Vam7, and HOPS (Fig. 4, *A* and *B*). Neither ATP nor Sec17 and Sec18 were required under these conditions (Fig. 4, *C* and *D*), as explained by the setup of our heterotypic fusion assay, where SNARE assembly is driven by the soluble Vam7. This shows that prenylated Ypt7 in its active state drives HOPS-dependent fusion with all previously established characteristics of content mixing.

Of the four required factors, each may support Rab localization to membranes. Conceptually, the GEF is the most upstream factor, as it activates the prenylated Rab and therefore allows for effector binding and prevents Rab extraction by GDI. GEFs should thus be able to time and localize a reaction cascade *in vivo*. To test this, we isolated the corresponding proteoliposomes after fusion. Prenylated Ypt7 was only found in the pellet of the liposome fraction, when Mon1–Ccz1 GEF was present (Fig. 4*E*, *lanes 8–10*). In the presence of GDP, little Ypt7 was bound (Fig. 4*E*, *lane 5*), whereas HOPS addition stabilized Ypt7 on membranes (Fig. 4*E*, *lanes 8* and *9*). Interestingly, HOPS

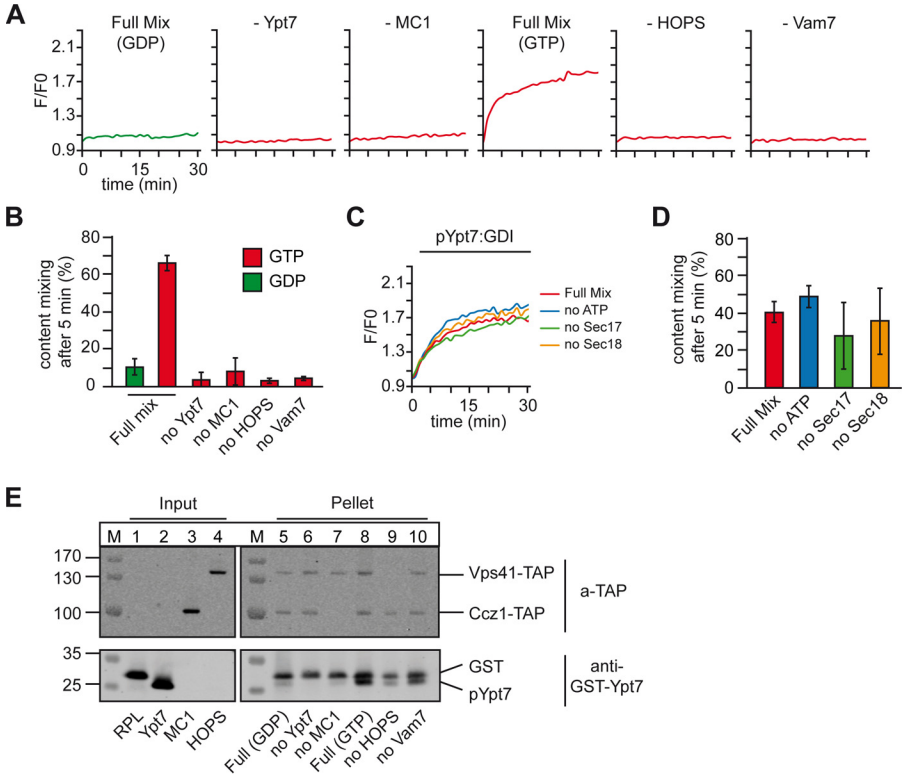

Figure 4. Reconstituted membrane fusion depends on membrane association and activation of Ypt7. *A* and *B*, fusion was performed in the presence of 80 nM pYpt7–GDI and either GDP or GTP and the full fusion mixture or in the absence of one of the components critical for fusion. *C* and *D*, controls of the heterotypic fusion reaction. Fusion was measured as in *A* with 80 nM Ypt7–GDI, leaving out either Sec17, Sec18, or ATP from the fusion mixture. *E*, fusion reactions after 30 min of fusion time as in *A* were fractionated by centrifugation for 30 min at 20,000 × *g*. Proteins in the pellet and supernatant were analyzed by SDS-PAGE and Western blotting, detecting the TAP tag on Vps41 and Ccz1, respectively, and Ypt7 ($n = 2$).

binding to membranes was also observed without Ypt7 but did not contribute to fusion (Fig. 4*E*, *top panel*). This indicates that Ypt7-binding may orient the HOPS for fusion on membranes. In agreement with these observations, we could completely limit fusion by sequentially titrating down Mon1–Ccz1 (Fig. 5*A*; quantified in Fig. 5*B*). Our data thus reveal that the GEF controls membrane localization and activation of prenylated Ypt7 and, thus, the entire fusion cascade.

Discussion

Here we uncover the minimal conditions under which organelle membranes can be made fusion-competent. Just four soluble factors are needed for Rab–GTP–dependent fusion: the GEF complex Mon1–Ccz1, the pYpt7–GDI complex, the HOPS tethering complex, and the SNARE Vam7. We demonstrate that the GEF is the most upstream factor limiting the fusion reaction by regulated spatiotemporal activation of pYpt7. Subsequently, HOPS interacts with membrane-bound pYpt7–GTP and triggers membrane fusion.

These observations agree with several *in vivo* and *in vitro* studies. GEF relocalization to mitochondria relocalizes the corresponding Rab as well (19, 20). Furthermore, the GEF complex TRAPP can only recruit and activate pYpt1–GDI on liposomes (21). We now extend these studies by embedding Rab activation into a fusion cascade that is entirely GEF-dependent.

We and others (21) did not find evidence that additional factors are required for dissociation of the Rab–GDI complex. However, we cannot exclude that additional factors facilitate this process *in vivo* to provide another layer of regulation; for instance, accelerated Rab membrane association. Indeed, Pra1 stimulates reconstituted Rab5-dependent fusion (18), and Pra1-mediated GDI displacement has been postulated to be a critical intermediate of Rab delivery (13–17). Other mechanisms, such as posttranslational modifications, may enhance GDI displacement and membrane recruitment of Rabs *in vivo* (36). At least Ypt7 and Vps21 efficiently partitioned by themselves into membranes out of the REP complex (Figs. 1 and 3*C*), and Ypt7 just requires Mon1–Ccz1 to be stabilized on membranes by nucleotide exchange in the presence of GDI (Figs. 3*C* and 4*E*), as observed for Ypt1 and Ypt32 in the presence of the TRAPP complexes (21).

In the context of Rab–effector interactions, GDI is critical to buffer any available Rab–GDP, making Rab–GTP the exclusive effector binding site on membranes. At least for Ypt7, we quantified the relative abundance of Rabs and effectors in the cell. Here the amount of available Rab appears to be limiting compared with the intracellular amount of effector proteins.[3] The main role of the GTPase-activating protein is then a constant shift of uncomplexed Rab–GTP to the GDI-extractable Rab–GDP form (5, 37). This, in turn, also strengthens the role of GDI in the cell by not only providing a membrane shuttling mechanism but also by giving higher specificity to membrane-bound Rab–GTP in terms of the Rab–effector interaction. The coop-

[3] P. Carpio Malia, L. Langemeyer, A. Perz, D. Kümmel, and C. Ungermann, unpublished observations.

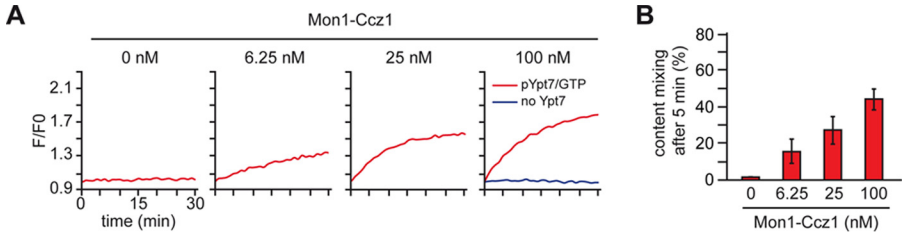

Figure 5. Mon1–Ccz1 drives activation of Ypt7 and, therefore, fusion. *A*, the amount of Mon1–Ccz1 was titrated down in the preincubation time of the fusion assay. As before, fusion was started after allowing for nucleotide exchange of 80 nM pYpt7–GDI for 15 min. *B*, quantification of two independent fusion reactions.

eration of GEF and GDI thus sharpens the boundaries between GDP- and GTP-bound forms (2, 5).

Previous work on the *Legionella* DrrA protein implied that the extraction of Rab from the GDI complex directly correlates with the GEF activity of the protein (38–41). Compared with intracellular GEFs, *Legionella* DrrA appears to be hyperactive and induces a dramatic conformational change to enforce efficient nucleotide exchange. This may be required for the pathogenicity of *Legionella* by restricting Rab1 to the *Legionella*-containing vacuole (39–41). Importantly, our work now extends these findings to intracellular GEFs such as the Mon1–Ccz1 complex.

Factors that regulate the membrane association of GEFs consequently have a strong impact on the correct spatiotemporal localization of effector proteins. For TRAPP, Arf1–GTP seems to be one critical factor (21); for Mon1–Ccz1, Rab5–GTP is a likely recruiter (42–46). Similarly, Mon1–Ccz1 localization will depend on corresponding membrane interactors, which need to be dissected in future experiments.

Importantly, GEFs so far require mainly peripheral membrane proteins for their binding, although membrane composition is likely also involved, such as phosphoinositides. This suggests that cytosolic proteins could sequentially recruit each other to a maturing organelle to complement the membrane-embedded SNARE proteins and thus specify fusion competence. We are confident that the dedicated orchestration of Rabs and their regulators can explain the principle of organelle maturation not only on endosomes but along the entire endomembrane system.

Materials and methods

Yeast strains

Strains overexpressing Mon1–Ccz1 and HOPS have been described previously (24, 29).

Expression and purification of Rab GTPases

GST-TEV-Ypt7 and GST-TEV-Vps21 were expressed and purified with slight modifications as described previously (24). Cells were lysed in a Microfluidizer (model M-110L, Microfluidics, Newton, MA), and the lysate was clarified by centrifugation at 40,000 × *g* for 30 min at 4 °C and loaded onto a pre-equilibrated Protino GST/4B 1-ml column (Macherey & Nagel). Protein was extensively washed and eluted in lysis buffer (50 mM Tris (pH 7.4), 300 mM NaCl, and 2 mM $MgCl_2$) containing either 20 mM glutathione or TEV protease for cleavage at 4 °C overnight. Proteins were then dialyzed into assay buffer (50 mM HEPES, NaOH (pH 7.4), 150 mM NaCl, and 2 mM $MgCl_2$), changing the buffer twice.

Expression and purification of Rab GGTase and Rab escort protein

pGATEV-Bet2 and pET30a-Bet4 (47) were co-expressed in *Escherichia coli* BL21 Rosetta, induced with 0.25 mM isopropyl 1-thio-β-D-galactopyranoside for 16 h at 18 °C. The Rab escort protein Mrs6 (48) was expressed and purified the same way. Cells were lysed in 50 mM Tris (pH 8.0), 300 mM NaCl, 2 mM β-mercaptoethanol, and 1 mM PMSF as described above. The cleared lysate was loaded on a Hi-Trap nickel-Sepharose column (GE Healthcare) equilibrated with the lysis buffer. The column was washed extensively with lysis buffer containing 30 mM imidazole, and bound protein was eluted with a linear 30 mM to 300 mM imidazole gradient over 30 column volumes. Fractions containing GGTase-II and REP, respectively, were pooled and dialyzed against assay buffer, which was changed twice.

Expression and purification of Gdi1

Competent *E. coli* Rosetta BL21 cells were transformed with pGEX-6P-Gdi1 (kindly provided by C. Fromme, Weill Institute, Cornell University). A single colony was picked from selection plates, and 2 liters of culture was grown to an A_{600} of around 0.8. Expression was induced with 0.25 mM isopropyl 1-thio-β-D-galactopyranoside, and cells were incubated at 18 °C overnight. Cells were lysed in PBS containing 1 mM PMSF, 2 mM $MgCl_2$, and 5 mM β-mercaptoethanol, and the cell homogenate was cleared as described above. Cleared lysate was loaded on a Protino GST/4B 1-ml column (Macherey & Nagel). Protein was eluted after extensive washing by cleaving the GST tag by incubating with Precision protease at 16 °C for 2 h.

Tandem affinity purification

Purifications were conducted essentially as described previously (29, 49). Three liters of culture were grown at 30 °C to A_{600}. Cells were harvested by centrifugation and lysed in buffer containing 50 mM HEPES-NaOH (pH 7.4), 150 mM NaCl, 1.5 mM $MgCl_2$, 1× Protease-Inhibitor-Mix FY (Serva), 0.5 mM PMSF, and 1 mM DTT. Lysates were centrifuged for 90 min at 100,000 × *g*, and supernatants were incubated with IgG-Sepharose (GE Healthcare) for 1.5 h at 4 °C. Beads were sedimented by centrifugation at 800 × *g* for 5 min and washed with 15 ml of lysis buffer containing 0.5 mM DTT. Bound proteins were eluted by TEV cleavage overnight and analyzed on SDS-PAGE.

In vitro prenylation of Rab GTPases

The assay was performed as described previously (50) with slight modifications. Equimolar amounts of GTPase preloaded with either GDP (Sigma-Aldrich) or MANT–GDP (Jena Bioscience) (51) and the Rab escort protein were incubated with a third of the amount of geranylgeranyl transferase and a 10-fold excess of geranylgeranyl pyrophosphate (Sigma-Aldrich, Munich, Germany) in assay buffer containing 1 mM DTT. The mixture was incubated at 37 °C for 30 min and used for subsequent assays. To obtain prenylated Ypt7–GDI, the prenylation reaction was performed as described previously (21).

Membrane association assay

Association of prenylated Rab GTPases to membranes was followed by incubation of 50 pmol of Rab GTPase with 50 nmol of liposomes (61 mol % palmitoyl-oleoyl-phosphatidylcholine, 18 mol % palmitoyl-oleoyl-phosphatidylethanolamine, 10 mol % palmitoyl-oleoyl-phosphatidylserine, 2 mol % phosphatidylinositol 3-phosphate, 8 mol % ergosterol, and 1 mol % diacylglycerol) (25) for 30 min at 30 °C. Liposomes were pelleted by centrifugation at 20,000 × *g* at 4 °C. Proteins in the supernatant and pellet fractions were separated and analyzed by SDS-PAGE and Coomassie staining.

Nucleotide exchange assays

GEF assays were performed as described previously (51). 50 pmol of MANT–GDP (Jena Bioscience)-loaded Rab GTPase was mixed with increasing amounts of GEF, and after baseline stabilization, exchange was triggered by addition of 0.1 mM GTP to the reaction. Nucleotide exchange was followed by measuring the decrease in fluorescence of the MANT fluorophore in a SpectraMax M3 multi-mode microplate reader (Molecular Devices). Where indicated, 50 nmol of liposomes was added to the reaction (25). Liposomes were composed as described above, and, where indicated, 10 mol % DOGS-NTA (1,2-dioleoyl-*sn*-glycero-3-[(*N*-(5-amino-1-carboxypentyl-)iminodiacetic acid)succinyl]) was added and compensated by reduction of the palmitoyl-oleoyl-phosphatidylcholine amount.

Fusion assay with reconstituted proteoliposomes (RPLs)

Fusion of RPLs, including purification of the involved proteins, was performed as described previously (26, 52) with the indicated protein-to-lipid ratios. One set of RPL carried Nyv1 and the other set Vti1 and Vam3. Where indicated, RPLs were preincubated with prenylated Rab-GTPase and 100 nM Mon1–Ccz1. The mixture was incubated for 15 min at 27 °C to allow for membrane association of the prenylated Rab–GTPase and nucleotide exchange. Where indicated, 500 nM Gdi1 was added afterward, and reactions were incubated for another 5 min before triggering fusion. Fusion was triggered by addition of 50 nM HOPS complex, 50 nM Sec18, 600 nM Sec17, and finally 100 nM Vam7. To follow full fusion of liposomes, content mixing and the subsequent increase in fluorescence were monitored in a SpectraMax M3 multi-mode microplate reader (Molecular Devices).

Fractionation of the RPL fusion assay

To test for membrane association in the RPL fusion assay, the fusion reaction containing pYpt7–GDI was followed in the SpectraMax M3 multi-mode microplate reader (Molecular Devices) as above for 45 min. Afterward, samples were transferred to centrifugation tubes and spun for 15 min at 20,000 × *g* and 4 °C. Pellet and supernatant fractions were separated, and the volume was adjusted to 500 μl with assay buffer containing 0.1% Triton X-100. Proteins were TCA-precipitated and subjected to SDS-PAGE followed by Western blotting. Proteins were detected using antibodies against GST-Ypt7 and the TAP tag antibody (Invitrogen, CAB1001) directed against the TAP tag at Vps41 and Ccz1, respectively.

Author contributions—C.U. conceived and coordinated the study and wrote the paper. L.L. performed all experiments, analyzed the data, and wrote the paper. A.P. purified several important proteins and established the prenylation assay with L.L. D.K. co-coordinated the study and wrote the paper. All authors reviewed the results and approved the final version of the manuscript.

Acknowledgments—We thank Michael Zick, William Wickner, Chris Fromme, Kirill Alexandrov, Roger Goody, and Stephan Kiontke for support, plasmids, and discussions.

References

1. Behnia, R., and Munro, S. (2005) Organelle identity and the signposts for membrane traffic. *Nature* **438,** 597–604 CrossRef Medline
2. Barr, F. A. (2013) Review series: Rab GTPases and membrane identity: causal or inconsequential? *J. Cell Biol.* **202,** 191–199 CrossRef Medline
3. Rak, A., Pylypenko, O., Niculae, A., Pyatkov, K., Goody, R. S., and Alexandrov, K. (2004) Structure of the Rab7:REP-1 complex: insights into the mechanism of Rab prenylation and choroideremia disease. *Br. J. Anaesth.* **117,** 749–760 Medline
4. Lachmann, J., Ungermann, C., and Engelbrecht-Vandré, S. (2011) Rab GTPases and tethering in the yeast endocytic pathway. *Small GTPases* **2,** 182–186 CrossRef Medline
5. Goody, R. S., Müller, M. P., and Wu, Y.-W. (2017) Mechanisms of action of Rab proteins, key regulators of intracellular vesicular transport. *Biol. Chem.* **398,** 565–575 CrossRef Medline
6. Pylypenko, O., Rak, A., Durek, T., Kushnir, S., Dursina, B. E., Thomae, N. H., Constantinescu, A. T., Brunsveld, L., Watzke, A., Waldmann, H., Goody, R. S., and Alexandrov, K. (2006) Structure of doubly prenylated Ypt1:GDI complex and the mechanism of GDI-mediated Rab recycling. *EMBO J.* **25,** 13–23 CrossRef Medline
7. Knödler, A., Feng, S., Zhang, J., Zhang, X., Das, A., Peränen, J., and Guo, W. (2010) Coordination of Rab8 and Rab11 in primary ciliogenesis. *Proc. Natl. Acad. Sci. U.S.A.* **107,** 6346–6351 CrossRef Medline
8. Ortiz, D., Medkova, M., Walch-Solimena, C., and Novick, P. (2002) Ypt32 recruits the Sec4p guanine nucleotide exchange factor, Sec2p, to secretory vesicles: evidence for a Rab cascade in yeast. *J. Cell Biol.* **157,** 1005–1015 CrossRef Medline
9. Mizuno-Yamasaki, E., Medkova, M., Coleman, J., and Novick, P. (2010) Phosphatidylinositol 4-phosphate controls both membrane recruitment and a regulatory switch of the Rab GEF Sec2p. *Dev. Cell* **18,** 828–840 CrossRef Medline
10. Poteryaev, D., Datta, S., Ackema, K., Zerial, M., and Spang, A. (2010) Identification of the switch in early-to-late endosome transition. *Cell* **141,** 497–508 CrossRef Medline
11. Rink, J., Ghigo, E., Kalaidzidis, Y., and Zerial, M. (2005) Rab conversion as a mechanism of progression from early to late endosomes. *Cell* **122,** 735–749 CrossRef Medline

12. Grosshans, B. L., Ortiz, D., and Novick, P. (2006) Rabs and their effectors: achieving specificity in membrane traffic. *Proc. Natl. Acad. Sci. U.S.A.* **103,** 11821–11827 CrossRef Medline
13. Dirac-Svejstrup, A. B., Sumizawa, T., and Pfeffer, S. R. (1997) Identification of a GDI displacement factor that releases endosomal Rab GTPases from Rab-GDI. *EMBO J.* **16,** 465–472 CrossRef Medline
14. Sivars, U., Aivazian, D., and Pfeffer, S. (2003) Yip3 catalyses the dissociation of endosomal Rab-GDI complexes. *Nature* **425,** 856–859 CrossRef Medline
15. Chen, C. Z., Calero, M., DeRegis, C. J., Heidtman, M., Barlowe, C., and Collins, R. N. (2004) Genetic analysis of yeast Yip1p function reveals a requirement for Golgi-localized rab proteins and rab-Guanine nucleotide dissociation inhibitor. *Genetics* **168,** 1827–1841 CrossRef Medline
16. Calero, M., Winand, N., and Collins, R. (2002) Identification of the novel proteins Yip4p and Yip5p as Rab GTPase interacting factors. *FEBS Lett.* **515,** 89–98 CrossRef Medline
17. Heidtman, M., Chen, C. Z., Collins, R. N., and Barlowe, C. (2005) Yos1p is a novel subunit of the Yip1p-Yif1p complex and is required for transport between the endoplasmic reticulum and the Golgi complex. *Mol. Biol. Cell* **16,** 1673–1683 CrossRef Medline
18. Ohya, T., Miaczynska, M., Coskun, U., Lommer, B., Runge, A., Drechsel, D., Kalaidzidis, Y., and Zerial, M. (2009) Reconstitution of Rab- and SNARE-dependent membrane fusion by synthetic endosomes. *Nature* **459,** 1091–1097 CrossRef Medline
19. Blümer, J., Rey, J., Dehmelt, L., Mazel, T., Wu, Y. W., Bastiaens, P., Goody, R. S., and Itzen, A. (2013) RabGEFs are a major determinant for specific Rab membrane targeting. *J. Cell Biol.* **200,** 287–300 CrossRef Medline
20. Gerondopoulos, A., Langemeyer, L., Liang, J.-R., Linford, A., and Barr, F. A. (2012) BLOC-3 mutated in Hermansky-Pudlak syndrome is a Rab32/38 guanine nucleotide exchange factor. *Curr. Biol.* **22,** 2135–2139 CrossRef Medline
21. Thomas, L. L., and Fromme, J. C. (2016) GTPase cross talk regulates TRAPPII activation of Rab11 homologues during vesicle biogenesis. *J. Cell Biol.* **215,** 499–513 CrossRef Medline
22. Thomä, N. H., Niculae, A., Goody, R. S., and Alexandrov, K. (2001) Double prenylation by RabGGTase can proceed without dissociation of the mono-prenylated intermediate. *J. Biol. Chem.* **276,** 48631–48636 CrossRef Medline
23. Pereira-Leal, J. B., Hume, A. N., and Seabra, M. C. (2001) Prenylation of Rab GTPases: molecular mechanisms and involvement in genetic disease. *FEBS Lett.* **498,** 197–200 CrossRef Medline
24. Nordmann, M., Cabrera, M., Perz, A., Bröcker, C., Ostrowicz, C., Engelbrecht-Vandré, S., and Ungermann, C. (2010) The Mon1-Ccz1 complex is the GEF of the late endosomal Rab7 homolog Ypt7. *Curr. Biol.* **20,** 1654–1659 CrossRef Medline
25. Cabrera, M., Nordmann, M., Perz, A., Schmedt, D., Gerondopoulos, A., Barr, F., Piehler, J., Engelbrecht-Vandré, S., and Ungermann, C. (2014) The Mon1-Ccz1 GEF activates the Rab7 GTPase Ypt7 via a longin-fold-Rab interface and association with PI3P-positive membranes. *J. Cell Sci.* **127,** 1043–1051 CrossRef Medline
26. Zucchi, P. C., and Zick, M. (2011) Membrane fusion catalyzed by a Rab, SNAREs, and SNARE chaperones is accompanied by enhanced permeability to small molecules and by lysis. *Mol. Biol. Cell* **22,** 4635–4646 CrossRef Medline
27. Zick, M., and Wickner, W. (2012) Phosphorylation of the effector complex HOPS by the vacuolar kinase Yck3p confers Rab nucleotide specificity for vacuole docking and fusion. *Mol. Biol. Cell* **23,** 3429–3437 CrossRef Medline
28. Mima, J., Hickey, C. M., Xu, H., Jun, Y., and Wickner, W. (2008) Reconstituted membrane fusion requires regulatory lipids, SNAREs and synergistic SNARE chaperones. *EMBO J.* **27,** 2031–2042 CrossRef Medline
29. Bröcker, C., Kuhlee, A., Gatsogiannis, C., Kleine Balderhaar, H. J., Hönscher, C., Engelbrecht-Vandré, S., Ungermann, C., and Raunser, S. (2012) Molecular architecture of the multisubunit homotypic fusion and vacuole protein sorting (HOPS) tethering complex. *Proc. Natl. Acad. Sci. U.S.A.* **109,** 1991–1996 CrossRef Medline
30. Hickey, C. M., and Wickner, W. (2010) HOPS initiates vacuole docking by tethering membranes before trans-SNARE complex assembly. *Mol. Biol. Cell* **21,** 2297–2305 CrossRef Medline
31. Orr, A., Wickner, W., Rusin, S. F., Kettenbach, A. N., and Zick, M. (2015) Yeast vacuolar HOPS, regulated by its kinase, exploits affinities for acidic lipids and Rab:GTP for membrane binding and to catalyze tethering and fusion. *Mol. Biol. Cell* **26,** 305–315 CrossRef Medline
32. Lürick, A., Gao, J., Kuhlee, A., Yavavli, E., Langemeyer, L., Perz, A., Raunser, S., and Ungermann, C. (2017) Multivalent Rab interactions determine tether-mediated membrane fusion. *Mol. Biol. Cell* **28,** 322–332 CrossRef Medline
33. Stroupe, C., Hickey, C. M., Mima, J., Burfeind, A. S., and Wickner, W. (2009) Minimal membrane docking requirements revealed by reconstitution of Rab GTPase-dependent membrane fusion from purified components. *Proc. Natl. Acad. Sci. U.S.A.* **106,** 17626–17633 CrossRef Medline
34. Zick, M., and Wickner, W. (2016) Improved reconstitution of yeast vacuole fusion with physiological SNARE concentrations reveals an asymmetric Rab(GTP) requirement. *Mol. Biol. Cell* **27,** 1–15 CrossRef Medline
35. Garrett, M. D., Zahner, J. E., Cheney, C., and Novick, P. J. (1994) GDI1 encodes a GDP dissociation inhibitor that plays an essential role in the yeast secretory pathway. *EMBO J.* **13,** 1718–1728 Medline
36. Oesterlin, L. K., Goody, R. S., and Itzen, A. (2012) Posttranslational modifications of Rab proteins cause effective displacement of GDP dissociation inhibitor. *Proc. Natl. Acad. Sci. U.S.A.* **109,** 5621–5626 CrossRef Medline
37. Dennis, M. K., Delevoye, C., Acosta-Ruiz, A., Hurbain, I., Romao, M., Hesketh, G. G., Goff, P. S., Sviderskaya, E. V., Bennett, D. C., Luzio, J. P., Galli, T., Owen, D. J., Raposo, G., and Marks, M. S. (2016) BLOC-1 and BLOC-3 regulate VAMP7 cycling to and from melanosomes via distinct tubular transport carriers. *J. Cell. Biol.* **214,** 293–308 CrossRef Medline
38. Machner, M. P., and Isberg, R. R. (2007) A bifunctional bacterial protein links GDI displacement to Rab1 activation. *Science* **318,** 974–977 CrossRef Medline
39. Schoebel, S., Oesterlin, L. K., Blankenfeldt, W., Goody, R. S., and Itzen, A. (2009) RabGDI displacement by DrrA from *Legionella* is a consequence of its guanine nucleotide exchange activity. *Mol. Cell* **36,** 1060–1072 CrossRef Medline
40. Suh, H.-Y., Lee, D.-W., Lee, K.-H., Ku, B., Choi, S.-J., Woo, J.-S., Kim, Y.-G., and Oh, B.-H. (2010) Structural insights into the dual nucleotide exchange and GDI displacement activity of SidM/DrrA. *EMBO J.* **29,** 496–504 CrossRef Medline
41. Zhu, Y., Hu, L., Zhou, Y., Yao, Q., Liu, L., and Shao, F. (2010) Structural mechanism of host Rab1 activation by the bifunctional *Legionella* type IV effector SidM/DrrA. *Proc. Natl. Acad. Sci. U.S.A.* **107,** 4699–4704 CrossRef Medline
42. Li, Y., Li, B., Liu, L., Chen, H., Zhang, H., Zheng, X., and Zhang, Z. (2015) FgMon1, a guanine nucleotide exchange factor of FgRab7, is important for vacuole fusion, autophagy and plant infection in *Fusarium graminearum*. *Sci. Rep.* **5,** 18101 Medline
43. Cui, Y., Zhao, Q., Gao, C., Ding, Y., Zeng, Y., Ueda, T., Nakano, A., and Jiang, L. (2014) Activation of the Rab7 GTPase by the MON1-CCZ1 complex is essential for PVC-to-vacuole trafficking and plant growth in *Arabidopsis*. *Plant Cell* **26,** 2080–2097 CrossRef Medline
44. Singh, M. K., Krüger, F., Beckmann, H., Brumm, S., Vermeer, J. E. M., Munnik, T., Mayer, U., Stierhof, Y.-D., Grefen, C., Schumacher, K., and Jürgens, G. (2014) Protein delivery to vacuole requires SAND protein-dependent Rab GTPase conversion for MVB-vacuole fusion. *Curr. Biol.* **24,** 1383–1389 CrossRef Medline
45. Kinchen, J. M., and Ravichandran, K. S. (2010) Identification of two evolutionarily conserved genes regulating processing of engulfed apoptotic cells. *Nature* **464,** 778–782 CrossRef Medline
46. Hegedűs, K, Takats, S., Boda, A., Jipa, A., Nagy, P., Varga, K., Kovacs, A. L., and Juhasz, G. (2016) The Ccz1-Mon1-Rab7 module and Rab5 control distinct steps of autophagy. *Mol. Biol. Cell* **27,** 3132–3142 CrossRef Medline

47. Kalinin, A., Thomä, N., Iakovenko, A., Heinemann, I., Rostkova, E., Constantinescu, A. T., and Alexandrov, K. (2001) Expression of mammalian geranylgeranyltransferase type-II in *Escherichia coli* and its application for *in vitro* prenylation of Rab proteins. *Protein Expr. Purif.* **22,** 84–91 CrossRef Medline
48. Pylypenko, O., Rak, A., Reents, R., Niculae, A., Sidorovitch, V., Cioaca, M. D., Bessolitsyna, E., Thomä, N. H., Waldmann, H., Schlichting, I., Goody, R. S., and Alexandrov, K. (2003) Structure of Rab escort protein-1 in complex with Rab geranylgeranyltransferase. *Mol. Cell* **11,** 483–494 CrossRef Medline
49. Ostrowicz, C. W., Bröcker, C., Ahnert, F., Nordmann, M., Lachmann, J., Peplowska, K., Perz, A., Auffarth, K., Engelbrecht-Vandré, S., and Ungermann, C. (2010) Defined subunit arrangement and rab interactions are required for functionality of the HOPS tethering complex. *Traffic* **11,** 1334–1346 CrossRef Medline
50. Wu, Y.-W., Tan, K.-T., Waldmann, H., Goody, R. S., and Alexandrov, K. (2007) Interaction analysis of prenylated Rab GTPase with Rab escort protein and GDP dissociation inhibitor explains the need for both regulators. *Proc. Natl. Acad. Sci. U.S.A.* **104,** 12294–12299 CrossRef Medline
51. Langemeyer, L., Nunes Bastos, R., Cai, Y., Itzen, A., Reinisch, K. M., and Barr, F. A. (2014) Diversity and plasticity in Rab GTPase nucleotide release mechanism has consequences for Rab activation and inactivation. *eLife* **3,** e01623 CrossRef Medline
52. Zick, M., and Wickner, W. T. (2014) A distinct tethering step is vital for vacuole membrane fusion. *eLife* **3,** e03251 CrossRef Medline